Supporting Information

Self-Assembled Heterometallic Complexes Showing Enhanced Two-Photon Absorption and Their Distribution in Living Cells

Qin Jiang[a,†], Xinda Yang[a,†], Pan Xiang[b], Marta Dudek[c], Katarzyna Matczyszyn[c,*], Marek Samoc[c], Xiaohe Tian[b,*], Yuhui Luo[a], Qiong Zhang[b,], Daqi Wang[d], Pengfei Shi[a,*]

[a]*School of Environmental and Chemical Engineering, Jiangsu Key Laboratory of Function Control Technology for Advanced Materials, Jiangsu Ocean University, Lianyungang 222005, China. shipf@jou.edu.cn.*

[b]*School of Life Science, Anhui University, Hefei 230039, China. xiaohe.t@ahu.edu.cn*

[c]*Advanced Materials Engineering and Modelling Group, Wroclaw University of Science and Technology, 50-370 Wroclaw, Poland.katarzyna.matczyszyn@pwr.edu.pl*

[d]*School of Chemistry, Liaocheng University, Liaocheng, 222005, China*

† These authors contributed equally.

CONTENT

Table S1. Crystallographic parameters of the complexes **1**-**4**.....3
Table S2. Selected bond lengths and bond angels of the complex **1**.....4
Table S3. Selected bond lengths and bond angels of the complex **2**.....5
Table S4. Selected bond lengths and bond angels of the complex **3**.....6
Table S5. Selected bond lengths and bond angels of the complex **4**.....7
Table S6. One-photon spectral data of complexes **1** to **6**.....8
Figure. S1 ORTEP drawing for complex **1**.....9
Figure. S2 ORTEP drawing for complex **2**.....9
Figure. S3 ORTEP drawing for complex **3**.....10
Figure. S4 ORTEP drawing for complex **4**.....10
Figure. S5 ^{1}H NMR spectrum of complex **1**.....11
Figure. S6 ^{1}H NMR spectrum of complex **2**.....11
Figure. S7 ^{1}H NMR spectrum of complex **4**.....12
Figure. S8 ^{1}H NMR spectrum of complex **5**.....12
Figure. S9 ^{1}H NMR spectrum of complex **3**.....13
Figure. S10 ^{1}H NMR spectrum of complex **6**.....13
Figure. S11 ESI-MS spectrum of complex **1**.....14
Figure. S12 ESI-MS spectrum of complex **2**.....14
Figure. S13 ESI-MS spectrum of complex **3**.....14
Figure. S14 UV-vis absorption spectra of the DPBF sensitized by complexes **1**-**6** 15
Figure. S15 Single-photon excited fluorescence spectra for complexes **1**-**6**.....15
Figure. S16 Co-localization experiments of complex **1** in Hela cells. 16
Figure. S17 Co-localization experiments of complex **2** in Hela cells. 16
Figure. S18 Co-localization experiments of complex **3** in Hela cells. 17
Figure. S19 Co-localization experiments of complex **4** in Hela cells. 17
Figure. S20 Co-localization experiments of complex **5** in Hela cells. 18
Figure. S21 Co-localization experiments of complex **6** in Hela cells. 18
In vitro cytotoxicity of complexes **1** to **6** in dark and under light irradiation. 19

Table S1. Crystallographic parameters of complexes 1-4

Complex	**1**	**2**	**3**	**4**
Empirical formula*	$C_{48}H_{62}F_{12}N_{10}P_2Ru\cdot$	$C_{53}H_{62}F_{12}N_{10}O_2P_2Ru$	$C_{40}H_{32}N_{10}O_8Zn$	$C_{62}H_{70}F_{24}N_{10}P_4\ O_5PtRu\cdot$
Formula weight	1282.08	1262.13	846.12	1911.32
T [K]	296(2) K	296(2) K	296(2)	298(2) K
Crystal system	Triclinic	Triclinic	Tetragonal	Orthorhombic
Space group	P-1	P-1	$P4_3$	Pnma
a [Å]	9.053(7)	9.179(3)	9.125(2)	28.21(2)
b [Å]	12.444(10)	12.056(4)	9.125(2)	59.04(4)
c [Å]	21.163(17)	21.623(7)	44.906(12)	8.65(7)
α [°]	84.573(13)	96.203(5)	90°	90°
β [°]	83.905(12)	99.507(5)	90°	90°
γ [°]	89.958(12)	92.535(5)	90°	90°
V/Å^3	2360(1)	2341.5(13)	3740(1)	1441.0(2)
Z	2	2	4	8
D calcd/(g·cm^{-3})	1.804	1.790	1.503	1.762
F(000)	1316	1296	1744	7600
Absorption coefficient	0.516 mm^{-1}	0.511 mm^{-1}	0.727 mm^{-1}	2.355 mm^{-1}
θ range	1.644~25.008°	2.051~27.764°	1.814~27.705°	2.571~25.019°
Reflections collected	11750	21914	22742	71293
independent reflections	8143	10770	8559	12790
GOF on F^2	1.002	1.005	1.018	0.982
R1 [I>2σ(I)]	0.1276	0.0657	0.0388	0.0882
wR_2 [I>2σ(I)]	0.3285	0.0886	0.0875	0.1158
CCDC	1940334	1940333	1940270	1957691

*Solvent molecules are included in the empirical formula

Table S2. **Selected bond lengths and bond angels for complex 1**

Bond Length(Å)			
Ru(1)-N(1)	2.00(10)	C(15)-N(3)	1.31(17)
Ru(1)-N(2)	2.01(12)	C(16)-N(4)	1.34(16)
Ru(1)-N(5)	2.03(9)	C(20)-N(4)	1.35(17)
Ru(1)-N(4)	2.10(10)	C(21)-N(5)	1.35(15)
Ru(1)-N(3)	2.10(14)	C(25)-N(5)	1.33(14)
Ru(1)-N(6)	2.10(10)	C(26)-N(6)	1.34(15)
C(1)-N(1)	1.33(16)	C(30)-N(6)	1.32(15)
C(5)-N(1)	1.42(16)	C(31)-N(7)	1.22(19)
C(6)-N(2)	1.40(17)	C(11)-N(3)	1.38(19)
C(10)-N(2)	1.37(19)	C(35)-N(7)	1.41(2)
Bond Angles/(º)			
N(1)-Ru(1)-N(2)	82.3(4)	N(5)-Ru(1)-N(3)	98.2(5)
N(1)-Ru(1)-N(5)	101.9(3)	N(4)-Ru(1)-N(3)	90.2(5)
N(2)-Ru(1)-N(5)	175.8(4)	N(1)-Ru(1)-N(6)	90.0(4)
N(1)-Ru(1)-N(4)	92.8(4)	N(2)-Ru(1)-N(6)	102.0(4)
N(2)-Ru(1)-N(4)	100.6(5)	N(5)-Ru(1)-N(6)	78.8(4)
N(5)-Ru(1)-N(4)	78.7(5)	N(4)-Ru(1)-N(6)	157.5(4)
N(1)-Ru(1)-N(3)	159.9(5)	N(3)-Ru(1)-N(6)	94.8(4)
N(2)-Ru(1)-N(3)	77.6(5)	C(11)-N(3)-Ru(1)	113.9(9)
C(1)-N(1)-Ru(1)	134.3(8)	C(20)-N(4)-Ru(1)	112.2(9)
C(5)-N(1)-Ru(1)	111.1(8)	C(16)-N(4)-Ru(1)	128.7(11)
C(10)-N(2)-Ru(1)	120.9(10)	C(21)-N(5)-Ru(1)	119.0(8)
C(6)-N(2)-Ru(1)	120.6(10)	C(25)-N(5)-Ru(1)	117.6(9)
C(15)-N(3)-Ru(1)	128.0(12)	C(30)-N(6)-Ru(1)	127.5(9)
C(26)-N(6)-Ru(1)	112.1(8)		

Table S3. **Selected bond lengths and bond angels for complex 2**

Bond Length(Å)			
Ru(1)-N(2)	1.98(3)	C(11)-N(3)	1.39(5)
Ru(1)-N(6)	1.99(3)	C(15)-N(3)	1.35(5)
Ru(1)-N(7)	2.05(3)	C(16)-N(4)	1.32(8)
Ru(1)-N(3)	2.05(4)	C(20)-N(4)	1.34(8)
Ru(1)-N(1)	2.05(4)	C(21)-N(7)	1.34(5)
Ru(1)-N(5)	2.04(4)	C(25)-N(7)	1.39(5)
C(1)-N(1)	1.34(5)	C(26)-N(6)	1.35(5)
C(5)-N(1)	1.37(5)	C(30)-N(6)	1.36(5)
C(6)-N(2)	1.35(5)	C(31)-N(5)	1.39(5)
C(10)-N(2)	1.35(5)	C(35)-N(5)	1.34(5)
Bond Angles/(º)			
N(6)-Ru(1)-N(2)	176.16(16)	C(1)-N(1)-Ru(1)	128.9(4)
N(6)-Ru(1)-N(5)	78.87(15)	C(5)-N(1)-Ru(1)	114.3(3)
N(2)-Ru(1)-N(5)	104.97(14)	C(10)-N(2)-Ru(1)	118.2(3)
N(6)-Ru(1)-N(3)	100.27(14)	C(6)-N(2)-Ru(1)	119.0(3)
N(2)-Ru(1)-N(3)	79.59(16)	C(15)-N(3)-Ru(1)	128.8(3)
N(5)-Ru(1)-N(3)	91.16(14)	C(11)-N(3)-Ru(1)	114.0(3)
N(6)-Ru(1)-N(1)	101.60(14)	C(35)-N(5)-Ru(1)	128.9(3)
N(2)-Ru(1)-N(1)	78.73(16)	C(31)-N(5)-Ru(1)	114.7(3)
N(5)-Ru(1)-N(1)	91.06(14)	C(26)-N(6)-Ru(1)	119.5(3)
N(3)-Ru(1)-N(1)	158.04(14)	C(30)-N(6)-Ru(1)	120.1(3)
N(6)-Ru(1)-N(7)	79.01(15)	C(25)-N(7)-Ru(1)	114.9(3)
N(2)-Ru(1)-N(7)	97.16(14)	C(21)-N(7)-Ru(1)	128.8(3)
N(5)-Ru(1)-N(7)	157.77(14)	N(1)-Ru(1)-N(7)	91.19(14)
N(3)-Ru(1)-N(7)	94.95(14)		

Table S4. **Selected bond lengths and bond angels for complex 3**

Bond lengths(Å)			
Zn(1)-N(4)	2.07(4)	C(15)-N(5)	1.33(7)
Zn(1)-N(8)	2.07(4)	C(16)-N(6)	1.29(9)
Zn(1)-N(5)	2.16(5)	C(20)-N(6)	1.35(9)
Zn(1)-N(9)	2.17(5)	C(21)-N(7)	1.32(7)
Zn(1)-N(3)	2.20(5)	C(25)-N(7)	1.34(6)
Zn(1)-N(7)	2.21(5)	C(26)-N(8)	1.32(7)
C(5)-N(3)	1.33(7)	C(31)-N(10)	1.32(10)
C(6)-N(4)	1.33(7)	C(35)-N(10)	1.29(10)
C(10)-N(4)	1.34(6)	C(36)-N(9)	1.36(6)
C(11)-N(5)	1.34(6)	C(40)-N(9)	1.33(7)
Bond Angles/(º)			
N(4)-Zn(1)-N(8)	169.51(16)	C(40)-N(9)-Zn(1)	126.8(4)
N(4)-Zn(1)-N(5)	76.31(15)	C(25)-N(7)-Zn(1)	113.4(3)
N(8)-Zn(1)-N(5)	110.58(16)	C(5)-N(3)-Zn(1)	114.6(4)
N(4)-Zn(1)-N(9)	111.44(17)	C(1)-N(3)-Zn(1)	126.1(4)
N(8)-Zn(1)-N(9)	76.56(16)	C(1)-N(3)-Zn(1)	126.1(4)
N(5)-Zn(1)-N(9)	94.30(18)	C(6)-N(4)-Zn(1)	119.5(3)
N(4)-Zn(1)-N(3)	75.38(16)	C(10)-N(4)-Zn(1)	118.5(3)
N(8)-Zn(1)-N(3)	97.74(17)	C(5)-N(3)-Zn(1)	114.6(4)
N(5)-Zn(1)-N(3)	151.61(15)	C(15)-N(5)-Zn(1)	126.5(4)
N(9)-Zn(1)-N(3)	94.04(18)	C(11)-N(5)-Zn(1)	115.3(3)
N(4)-Zn(1)-N(7)	96.40(17)	C(36)-N(9)-Zn(1)	114.3(3)
N(8)-Zn(1)-N(7)	75.60(16)	C(15)-N(5)-Zn(1)	126.5(4)
N(5)-Zn(1)-N(7)	93.88(18)	C(21)-N(7)-Zn(1)	127.4(4)
N(9)-Zn(1)-N(7)	152.11(15)	C(25)-N(7)-Zn(1)	113.4(3)
N(3)-Zn(1)-N(7)	91.28(17)	C(10)-N(4)-Zn(1)	118.5(3)
C(11)-N(5)-Zn(1)	115.3(3)	C(26)-N(8)-Zn(1)	118.9(3)
C(21)-N(7)-Zn(1)	127.4(4)	C(30)-N(8)-Zn(1)	118.4(3)

Table S5. **Selected bond lengths and bond angels for complex 4**

Bond lengths(Å)			
Pt(1)-N(9)	1.98(9)	N(3)-C(15)	1.41(14)
Pt(1)-N(10)	2.02(13)	N(4)-C(20)	1.31(13)
Pt(1)-N(4)	2.04(9)	N(4)-C(16)	1.36(14)
Pt(1)-N(8)	2.08(12)	N(5)-C(21)	1.43(17)
Ru(1)-N(6)	1.96(11)	N(5)-C(25)	13.5(16)
Ru(1)-N(2)	1.99(11)	N(6)-C(30)	1.40(18)
Ru(1)-N(3)	2.05(10)	N(6)-C(26)	1.43(16)
Ru(1)-N(5)	2.01(13)	N(7)-C(35)	1.39(15)
Ru(1)-N(7)	2.05(11)	N(7)-C(31)	1.37(17)
Ru(1)-N(1)	2.10(9)	N(8)-C(36)	1.35(14)
N(1)-C(1)	1.33(13)	N(8)-C(40)	1.40(17)
N(1)-C(5)	1.43(15)	N(9)-C(41)	1.32(15)
N(2)-C(6)	1.38(14)	N(9)-C(45)	1.35(13)
N(2)-C(10)	1.36(14)	N(10)-C(46)	1.27(15)
N(3)-C(11)	1.35(14)	N(10)-C(50)	1.34(15)
Bond Angles/(º)			
N(9)-Pt(1)-N(10)	79.6(5)	C(1)-N(1)-Ru(1)	127.0(9)
N(9)-Pt(1)-N(4)	178.1(5)	C(5)-N(1)-Ru(1)	115.7(9)
N(10)-Pt(1)-N(4)	99.3(5)	C(6)-N(2)-Ru(1)	117.3(10)
N(9)-Pt(1)-N(8)	82.7(5)	C(10)-N(2)-Ru(1)	118.9(10)
N(10)-Pt(1)-N(8)	162.3(6)	C(11)-N(3)-Ru(1)	117.4(10)
N(4)-Pt(1)-N(8)	98.5(5)	C(15)-N(3)-Ru(1)	125.8(9)
N(6)-Ru(1)-N(2)	178.7(5)	C(20)-N(4)-Pt(1)	123.9(10)
N(6)-Ru(1)-N(3)	102.2(5)	C(16)-N(4)-Pt(1)	119.2(10)
N(2)-Ru(1)-N(3)	77.2(5)	C(21)-N(5)-Ru(1)	122.9(12)
N(6)-Ru(1)-N(5)	79.0(6)	C(25)-N(5)-Ru(1)	117.3(13)
N(2)-Ru(1)-N(5)	99.9(6)	C(30)-N(6)-Ru(1)	120.3(11)
N(3)-Ru(1)-N(5)	94.9(4)	C(26)-N(6)-Ru(1)	118.4(12)
N(6)-Ru(1)-N(7)	77.7(6)	C(35)-N(7)-Ru(1)	128.5(10)
N(2)-Ru(1)-N(7)	103.5(4)	C(31)-N(7)-Ru(1)	114.4(12)
N(3)-Ru(1)-N(7)	91.2(4)	C(36)-N(8)-Pt(1)	129.0(11)
N(5)-Ru(1)-N(7)	156.6(6)	C(40)-N(8)-Pt(1)	108.8(12)
N(6)-Ru(1)-N(1)	101.1(4)	C(41)-N(9)-Pt(1)	115.1(11)
N(2)-Ru(1)-N(1)	79.4(5)	C(45)-N(9)-Pt(1)	115.0(10)
N(3)-Ru(1)-N(1)	156.6(5)	C(46)-N(10)-Pt(1)	114.7(12)
N(5)-Ru(1)-N(1)	87.1(4)	C(50)-N(10)-Pt(1)	124.0(10)
N(7)-Ru(1)-N(1)	96.2(4)		

Complex	UV−vis, λ ($\varepsilon \times 10^4$)[a]	λ_{ex} (nm)[b]	λ_{em} (nm)[b]	$10^3\,\Phi$[c]	τ(ns)[c]	χ^2
1	490(1.71), 315(4.32), 278(3.93)	469	654	0.0008	0.018	1.39
2	494(2.02), 312(5.44), 276(4.29)	467	665	0.0022	0.043	1.74
3	324(3.31), 281(5.13)	310	360	0.6859	-	-
4	489(1.86), 315(5.71), 277(4.60)	495	685	0.0064	1.26	1.47
5	494(1.80), 312(5.63), 277(3.59)	493	693	0.0059	1.02	1.39
6	332(2.49), 280(6.58)	310	370	0.0937	-	-

Table S6. One-photon spectral data of complexes **1** to **6**. [a]UV−vis were measured in DMSO. [b]Represent the maximum excitation and emission wavelengths respectively. [c]One-photon fluorescence data were measured in water.

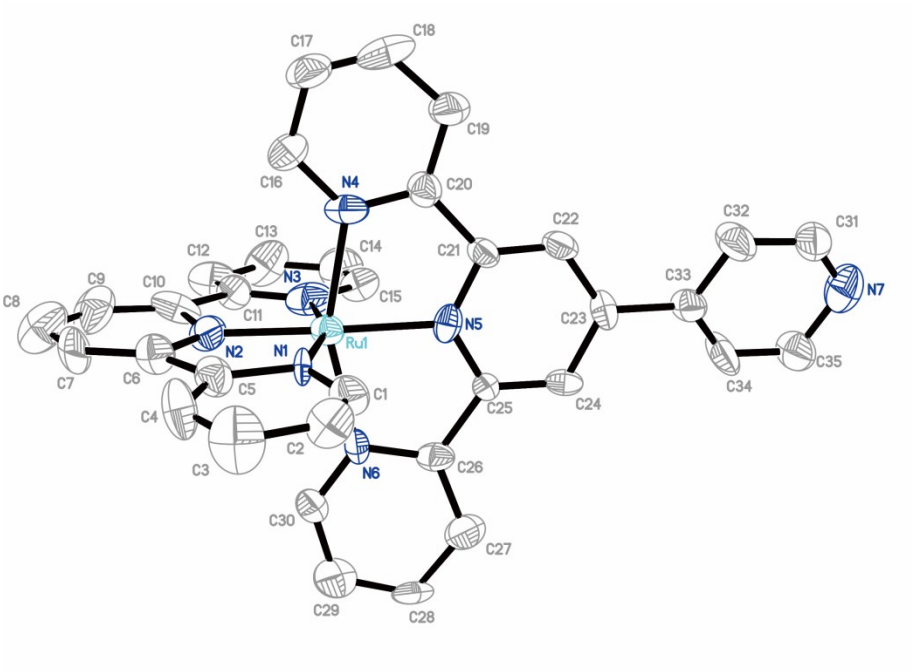

Figure S1. ORTEP drawing with 30% ellipse probability for complex **1**. H atoms and anions were omitted for clarity.

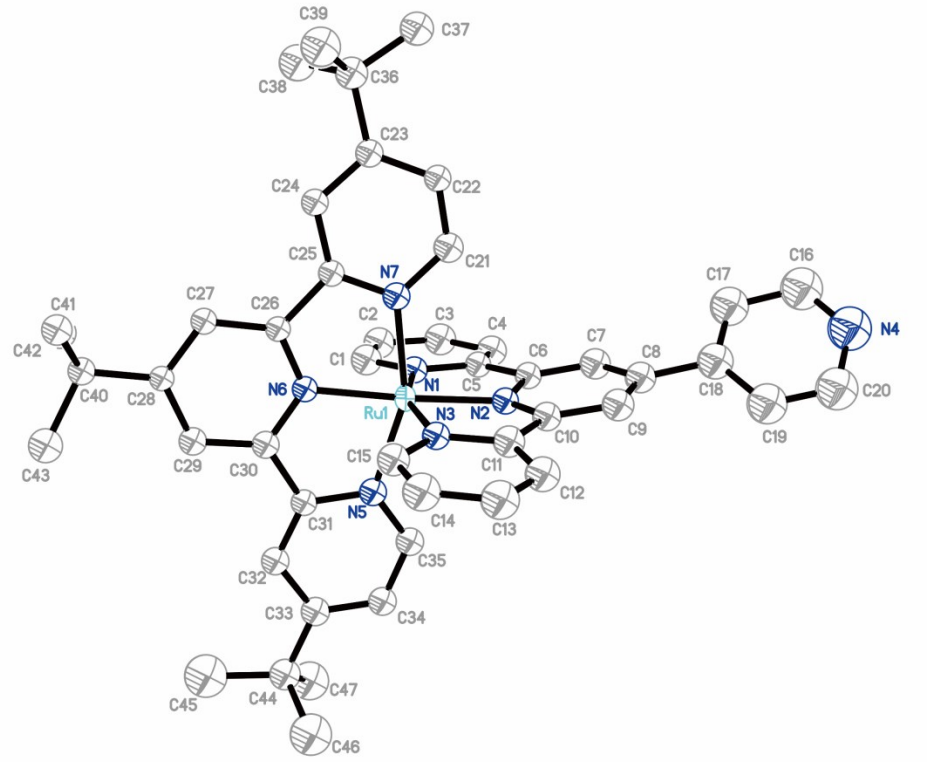

Figure S2. ORTEP drawing with 30% ellipse probability for complex **2**. H atoms and anions were omitted for clarity.

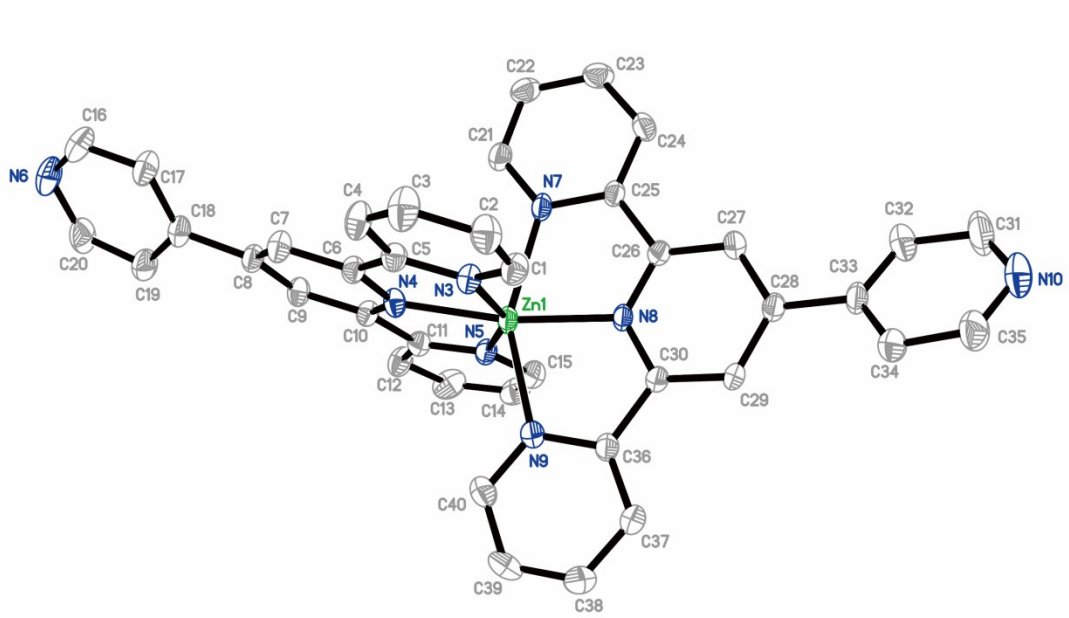

Figure S3. ORTEP drawing with 30% ellipse probability for complex **3**. H atoms and anions were omitted for clarity.

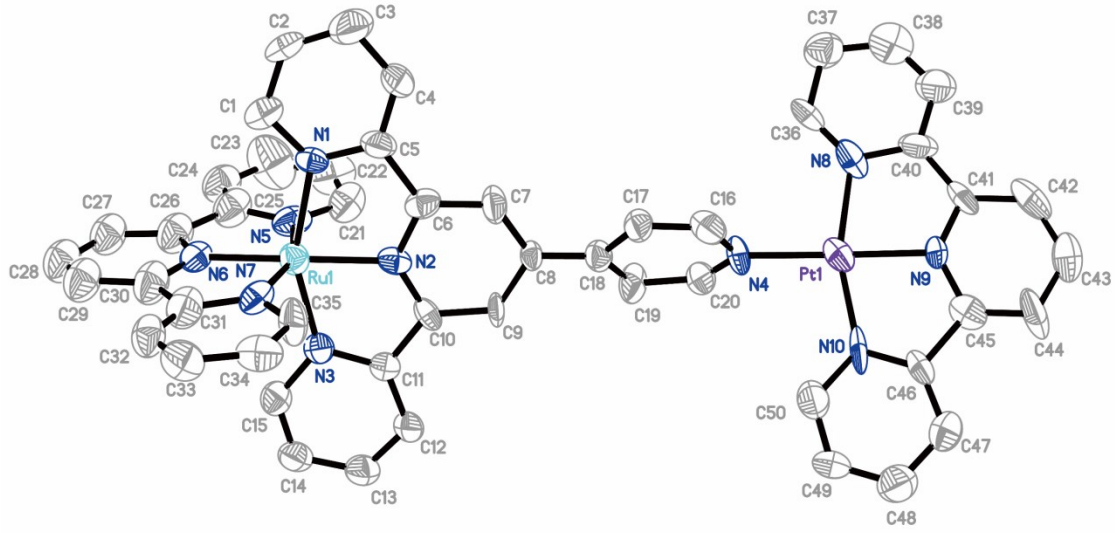

Figure S4. ORTEP drawing with 30% ellipse probability for complex **4**. H atoms and anions were omitted for clarity.

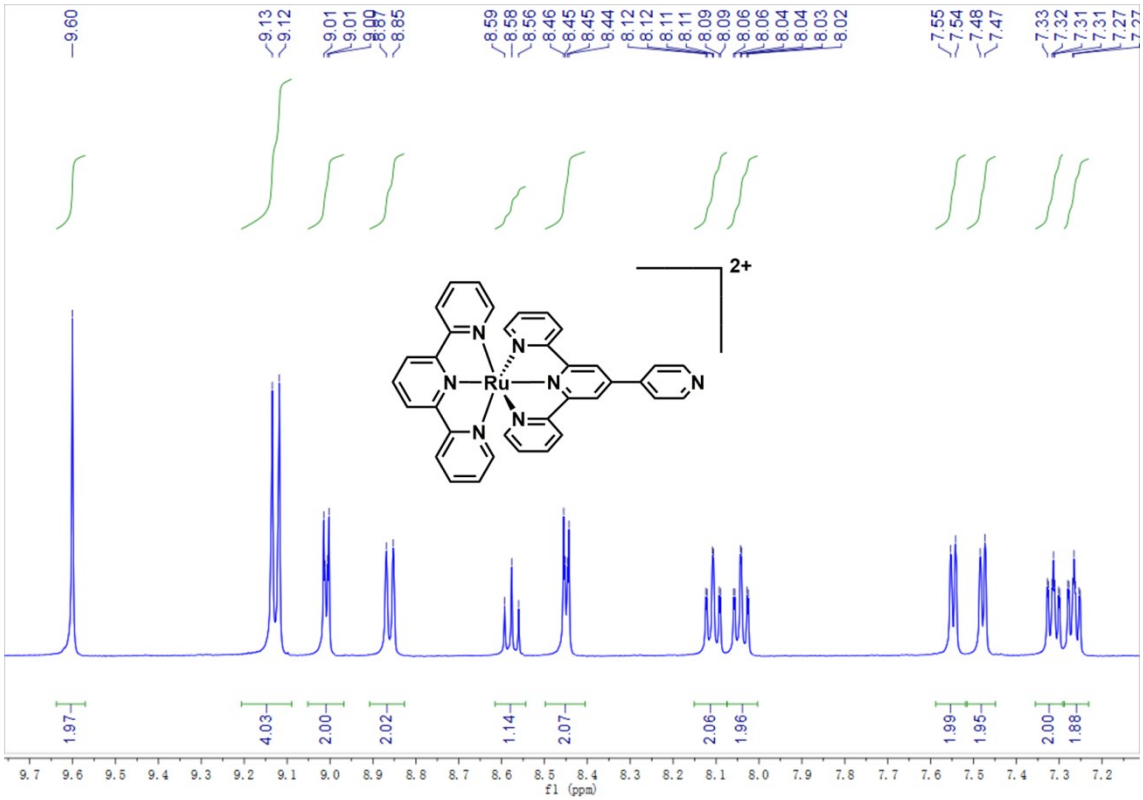

Figure S5. ^{1}H NMR spectrum (500 MHz, d_6-DMSO) of complex **1**.

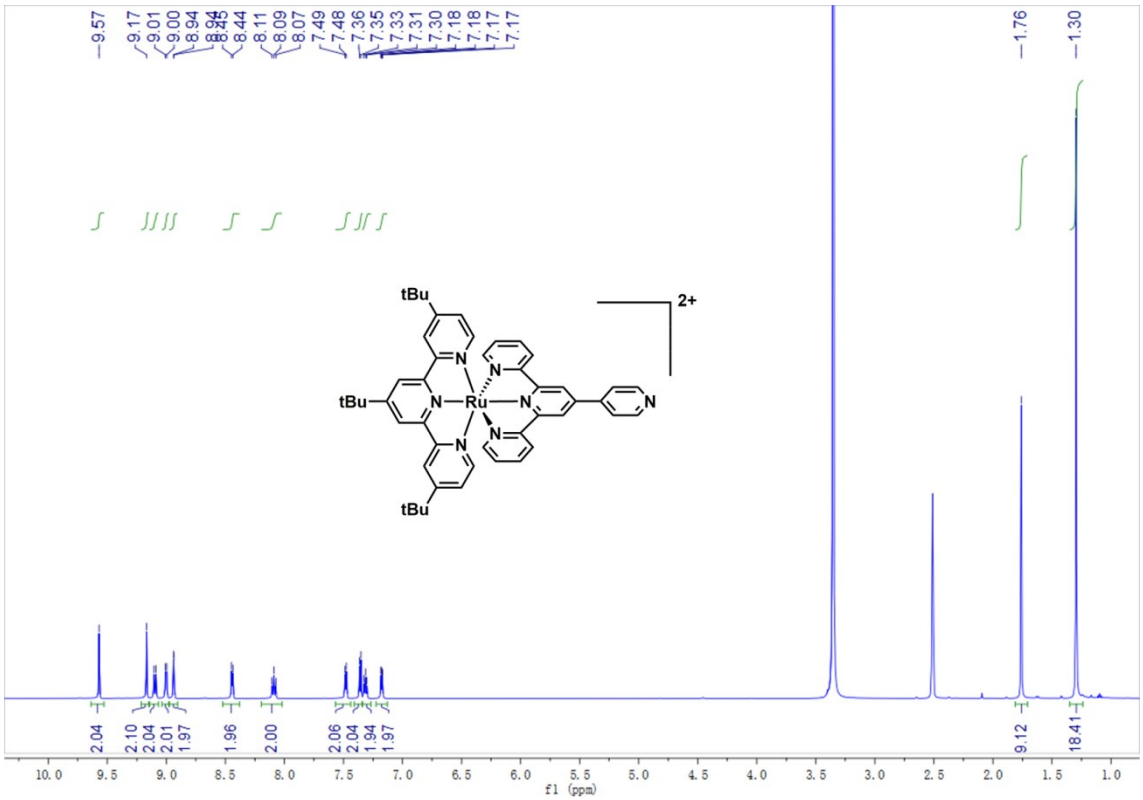

Figure S6. ^{1}H NMR spectrum (500 MHz, d_6-DMSO) of complex **2**.

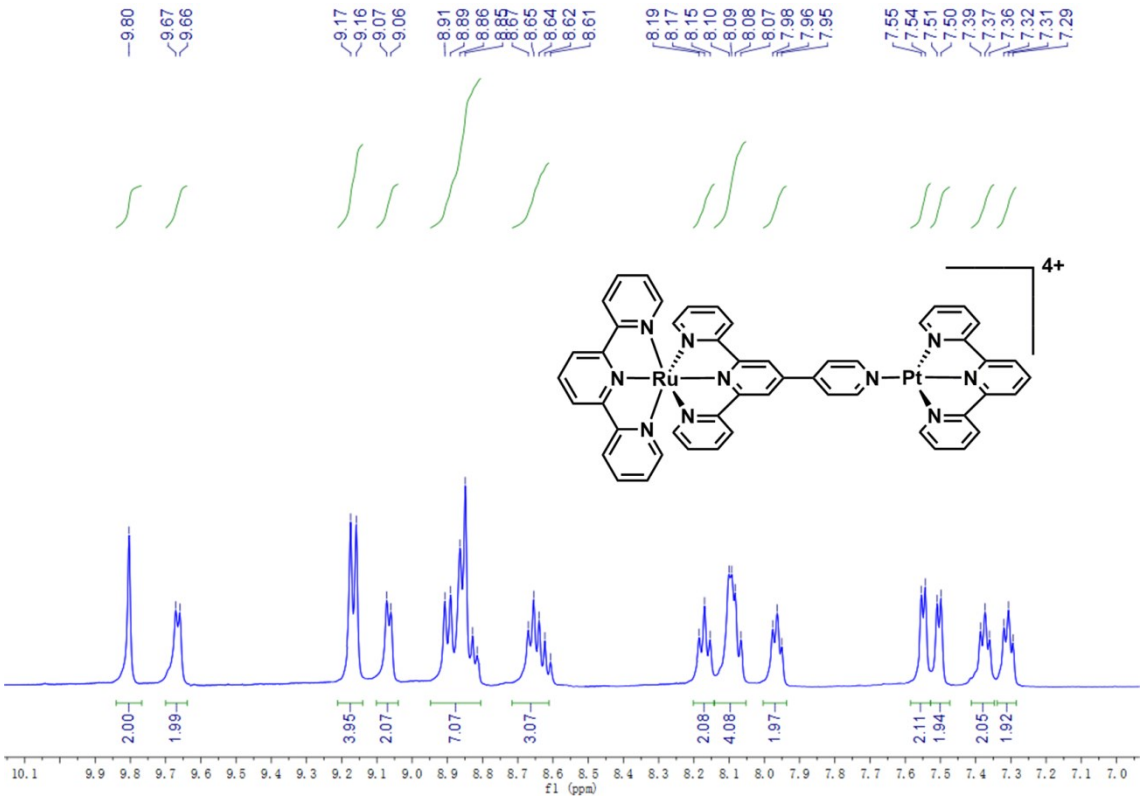

Figure S7. ^{1}H NMR spectrum (500 MHz, d_6-DMSO) of complex **4**.

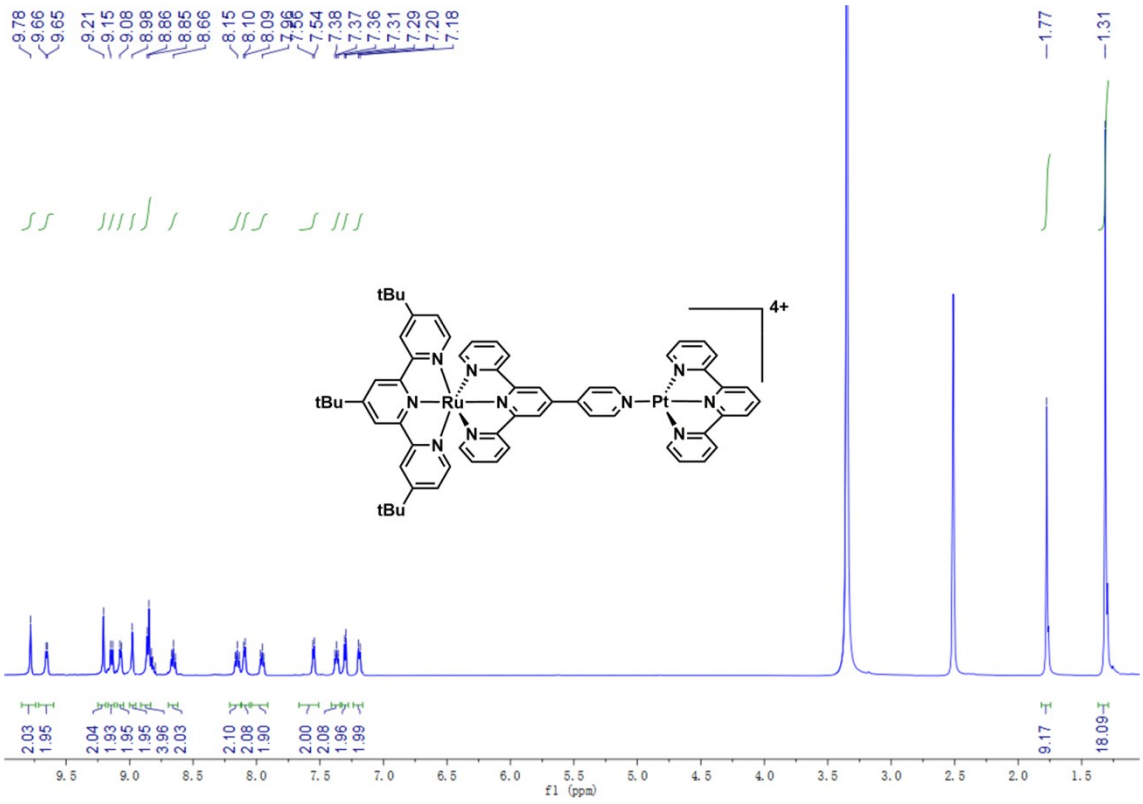

Figure S8. ^{1}H NMR spectrum (500 MHz, d_6-DMSO) of complex **5**.

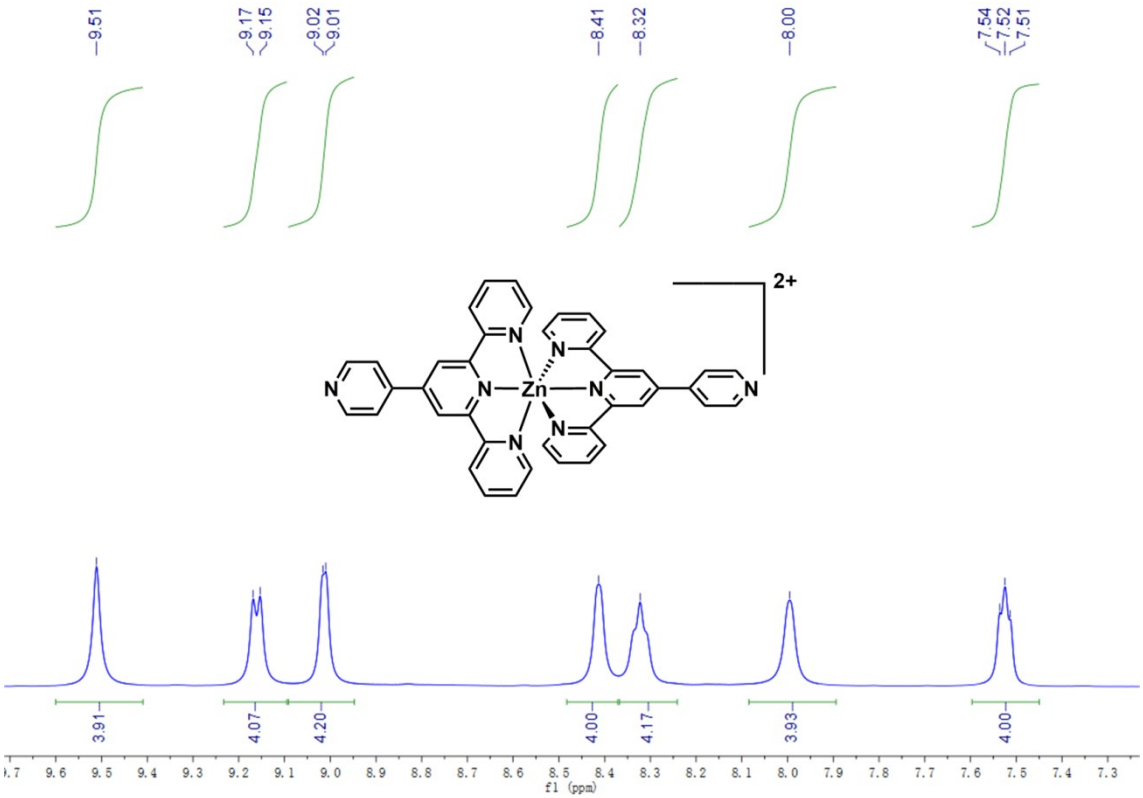

Figure S9. ^{1}H NMR spectrum (500 MHz, d_6-DMSO) of complex **3**.

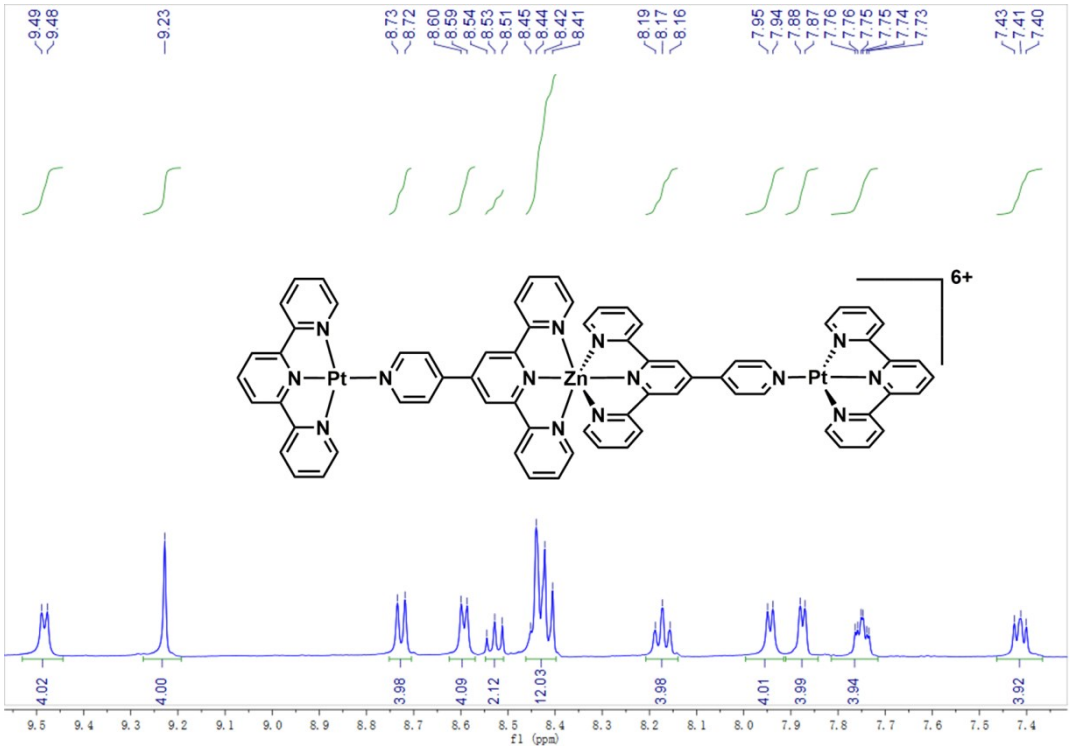

Figure S10. ^{1}H NMR spectrum (500 MHz, D_2O) of complex **6**.

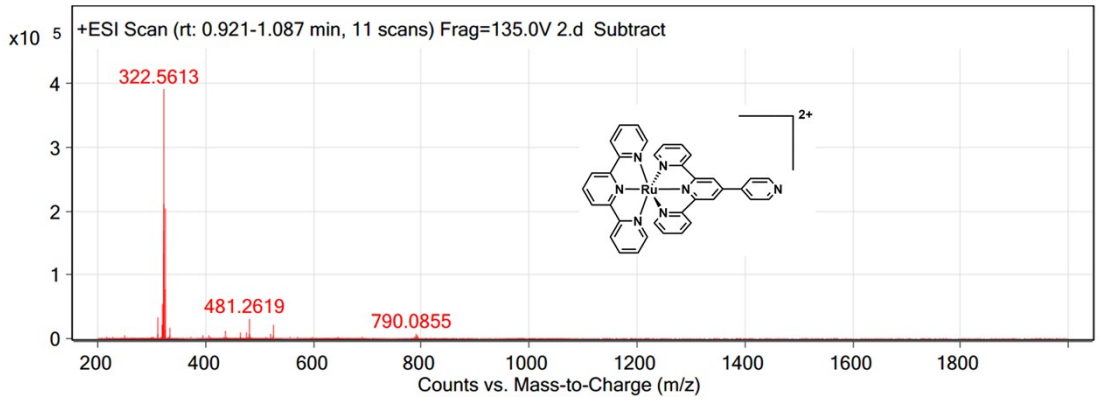

Figure S11. ESI-MS spectrum of complex **1**.

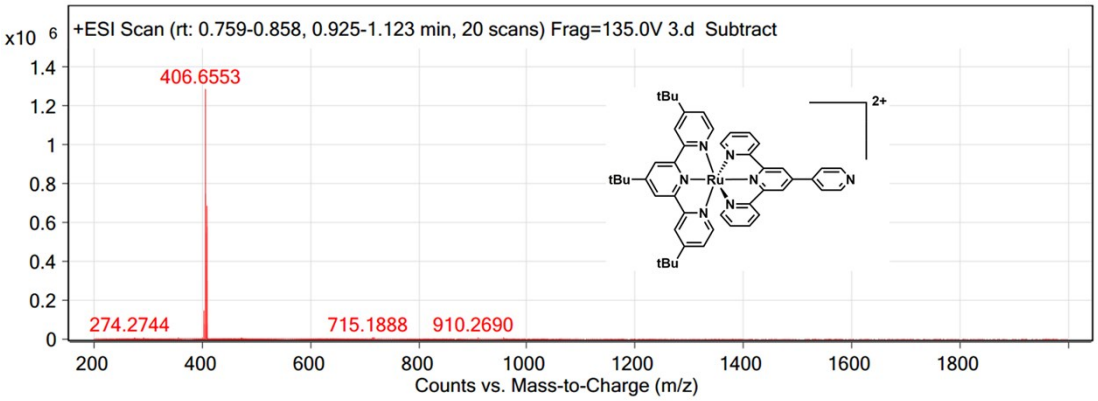

Figure S12. ESI-MS spectrum of complex **2**.

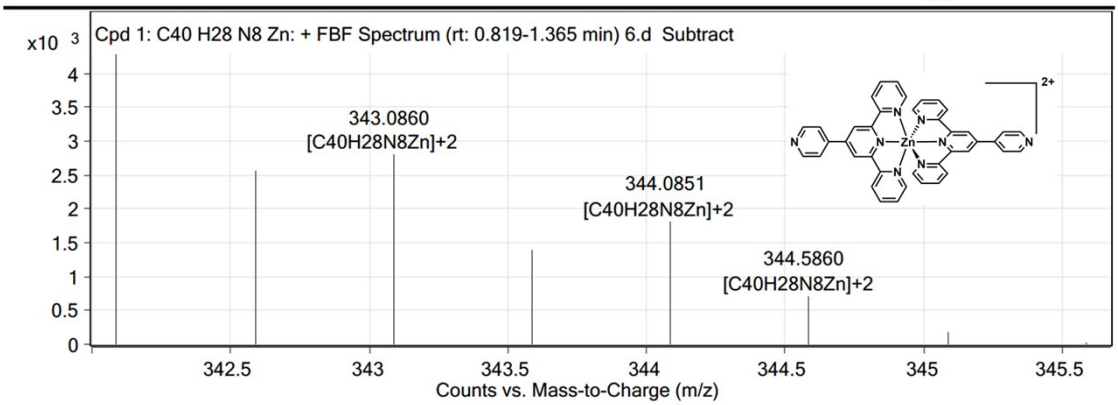

Figure S13. ESI-MS spectrum of complex **3**.

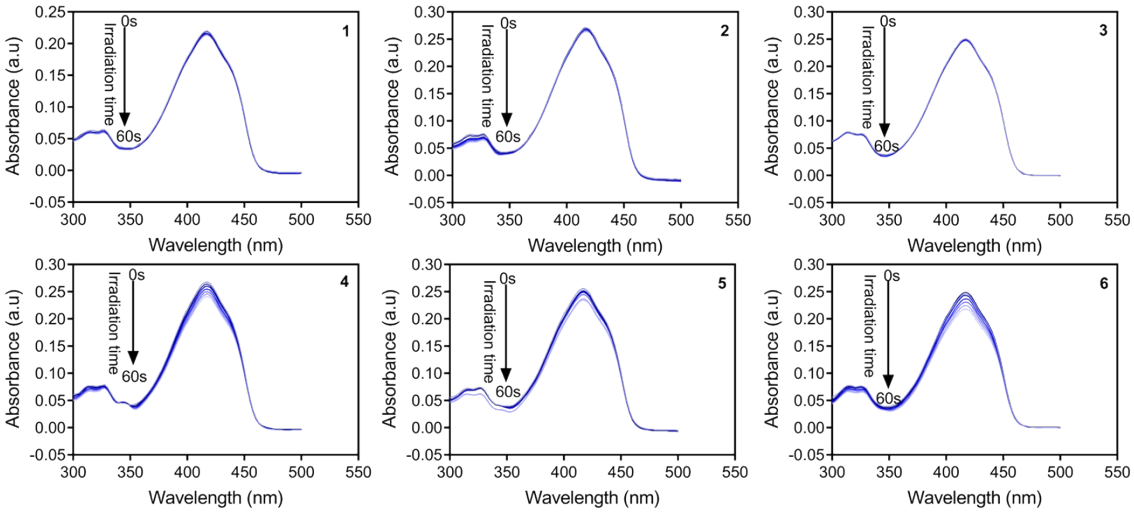

Figure S14. UV-vis absorption spectra of the DPBF (initial concentration = 10 μM) sensitized by complexes **1-6** in aerated DMSO. The absorbance of DPBF at 418 nm was recorded every 10 s.

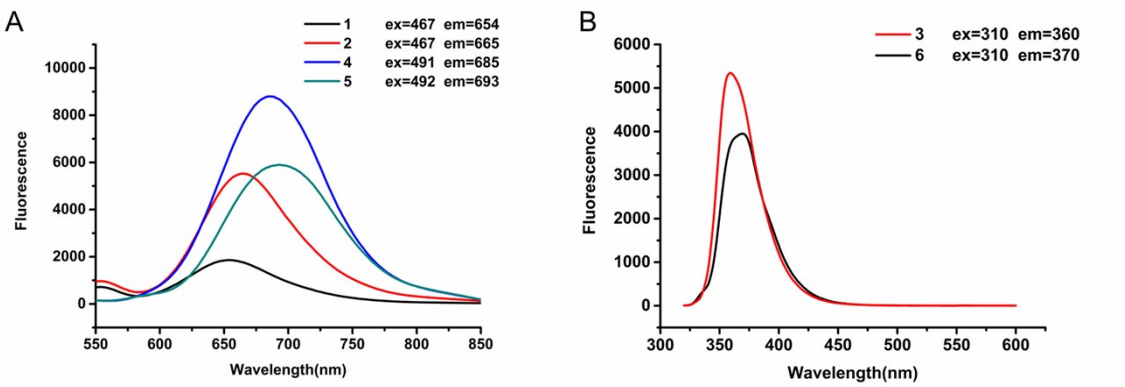

Figure S15. Single-photon excited fluorescence spectra for complexes **1**, **2**, **4**, **5** in H_2O solution. ($c=1.0\times10^{-5}$ mol/L. A). Single-photon excited fluorescence spectra for complexes **3**, **6** in H_2O solution. ($c=1.0\times10^{-5}$ mol/L, B)

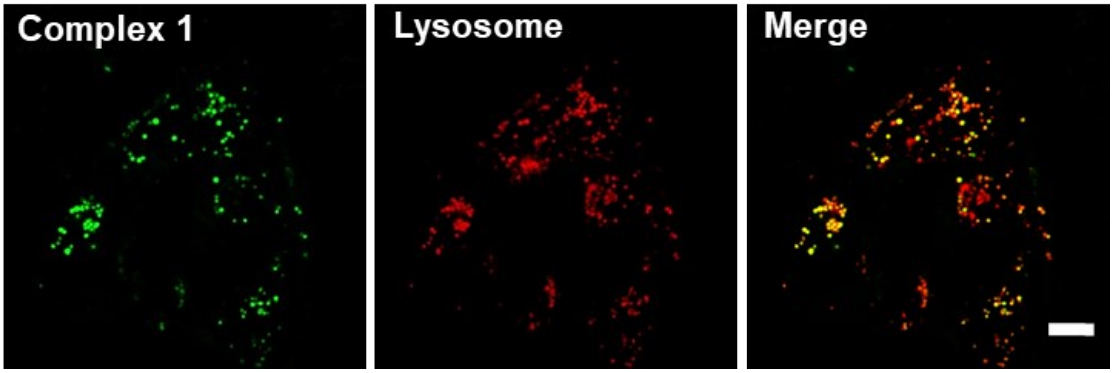

Figure. S16. Co-localization experiments involving complex **1** and Lyso Tracker Red (LTR) in Hela cells. The cells were incubated with LTR (1 μM) for 8 min and incubated with complex **1** (5 μM) upon dark environment for 5 min. Confocal images from complex **1** (ex = 405 nm) and LTR (ex = 594 nm) were on One-Photon Channel. Scale bar = 5 μm.

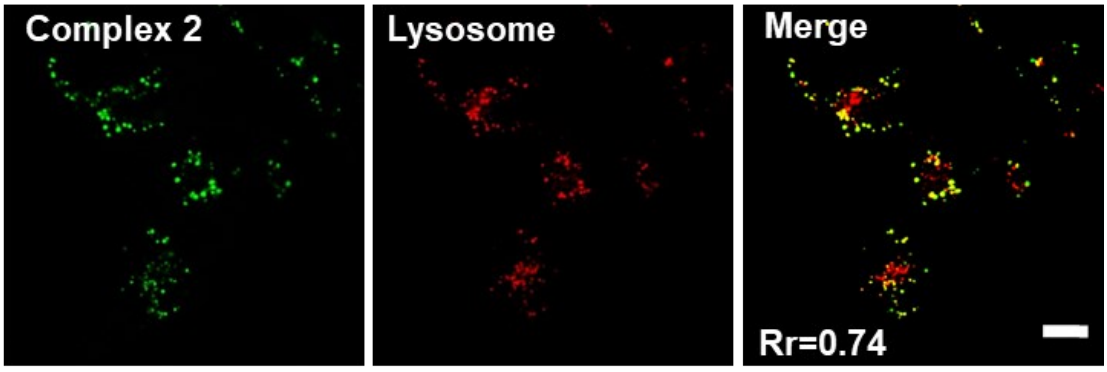

Figure. S17. Co-localization experiments involving complex **2** and Lyso Tracker Red (LTR) in Hela cells. The cells were incubated with LTR (1 μM) for 8 min and incubated with complex **2** (5 μM) upon dark environment for 5 min. Confocal images from complex **2** (ex = 405 nm) and LTR (ex = 594 nm) were on One-Photon Channel. Scale bar = 5 μm.

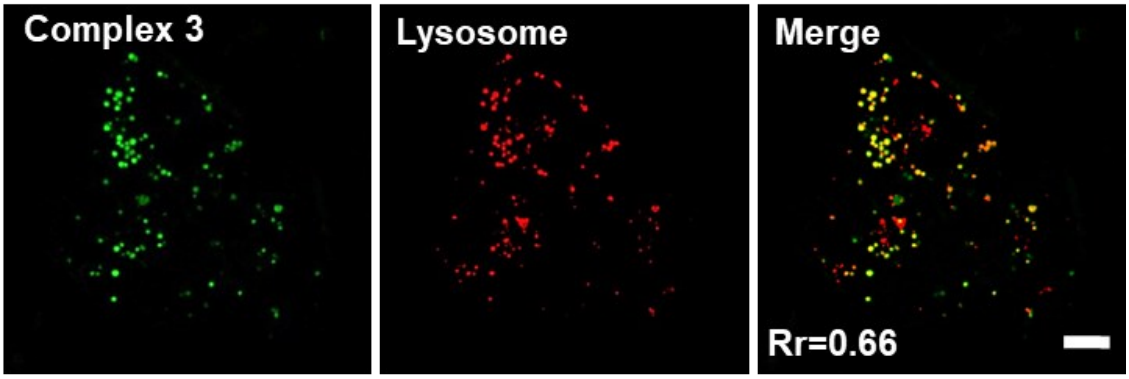

Figure. S18. Co-localization experiments involving complex **3** and Lyso Tracker Red (LTR) in Hela cells. The cells were incubated with LTR (1 μM) for 8 min and incubated with complex **3** (5 μM) upon dark environment for 5 min. Confocal image from complex **3** (ex = 405 nm) and LTR (ex = 594 nm) were on One-Photon Channel. Scale bar = 5 μm.

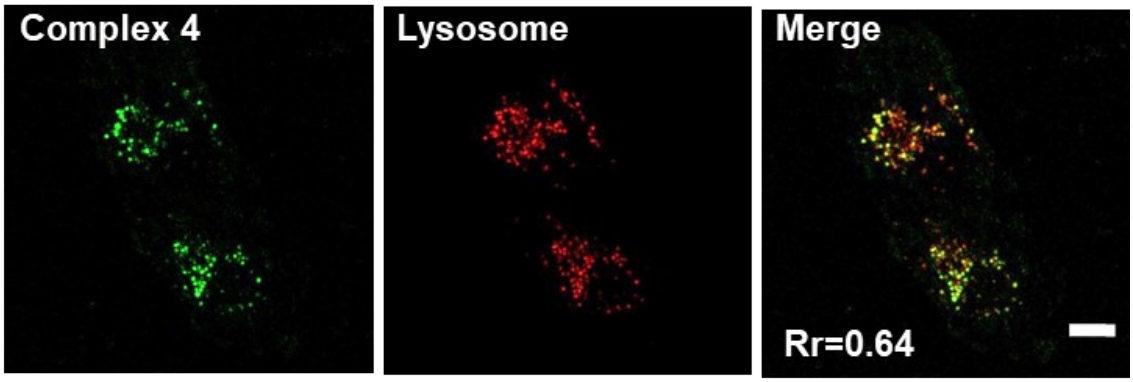

Figure. S19. Co-localization experiments involving complex **4** and Lyso Tracker Red (LTR) in Hela cells. The cells were incubated with LTR (1 μM) for 8 min and incubated with complex **4** (5 μM) upon dark environment for 5 min. Confocal images from complex **4** (ex = 405 nm) and LTR (ex = 594 nm) were on One-Photon Channel. Scale bar = 5 μm.

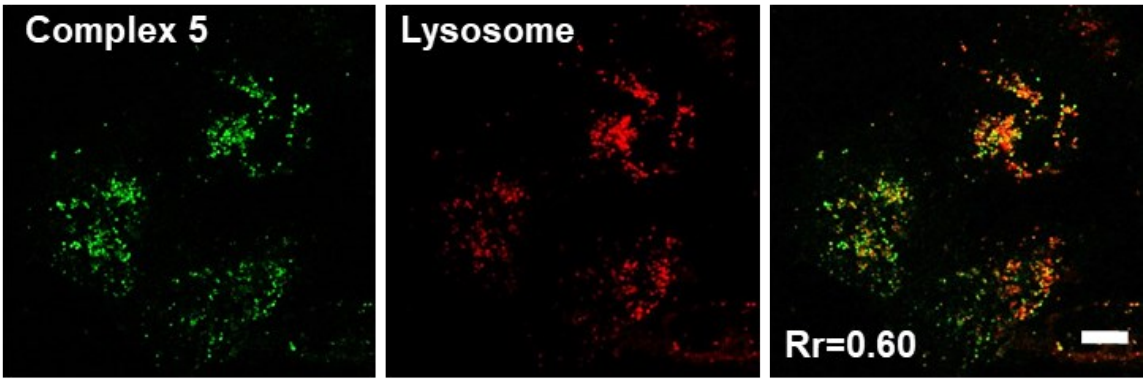

Figure. S20. Co-localization experiments involving complex **5** and Lyso Tracker Red (LTR) in Hela cells. The cells were incubated with LTR (1 μM) for 8 min and incubated with complex **5** (5 μM) upon dark environment for 5 min. Confocal images from complex **5** (ex = 405 nm) and LTR (ex = 594 nm) were on One-Photon Channel. Scale bar = 5 μm.

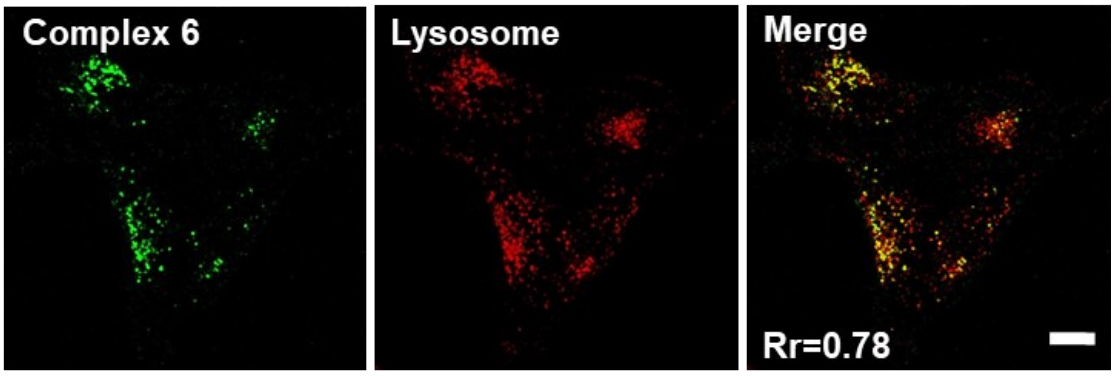

Figure. S21. Co-localization experiments involving complex **6** and Lyso Tracker Red (LTR) in Hela cells. The cells were incubated with LTR (1 μM) for 8 min and incubated with complex **6** (5 μM) upon dark environment for 5 min. Confocal images from complex **6** (ex = 405 nm) and LTR (ex = 594 nm) were on One-Photon Channel. Scale bar = 5 μm.

In vitro cytotoxicity of complexes 1 to 6 in dark and under light irradiation

Considering that Ru-Pt and Zn-Pt complex exhibited a certain ability to generate $^1O_2$ under cell-free conditions, we evaluated the vitro cytotoxicity of complexes **1**-**6** against HeLa cell lines via MTT assay in dark and under light irradiation (**Fig. S22**). All the platinization derivatives exhibited decreased IC_{50} values when compared with the corresponding Ru^{II} or Zn^{II} precursors in the absence of light (**Table S7**), indicating that Pt^{II}(tpy) fragments evidently improve the cytotoxicity of the Ru-Pt or Zn-Pt complexes. However, when irradiated with 365 nm ultraviolet light for 30 min, the IC_{50} values for **4** and **5** increased unexpectedly while complex **6** displayed prominent photocytotoxicity. We suggested that the increased IC_{50} values for **4** and **5** may be attributed to the cellular stress response (CSR) generated under the irradiation by ultraviolet light[1,2]. It can be observed from the data that metal centres have great impact on the cytotoxic activity of the heterometallic complexes, as can be seen from the different IC_{50} values of Zn-Pt and Ru-Pt complexes.

Table S7 Dark- and Photo-Toxicity[a] of complexes **1** to **6** toward HeLa Cells.

	HeLa cells		
complex	**dark**	**light**	**PI**[b]
1	42.80	37.6	1.14
2	40.20	29.93	1.34
4	25.01	59.40	<1
5	27.30	42.09	<1
3	150.90		
6	139.2	31.43	4.43

[a]IC_{50} values were an average of three measurements(μmol/L).
[b]PI, which is the ratio of dark IC_{50} and light IC_{50} values

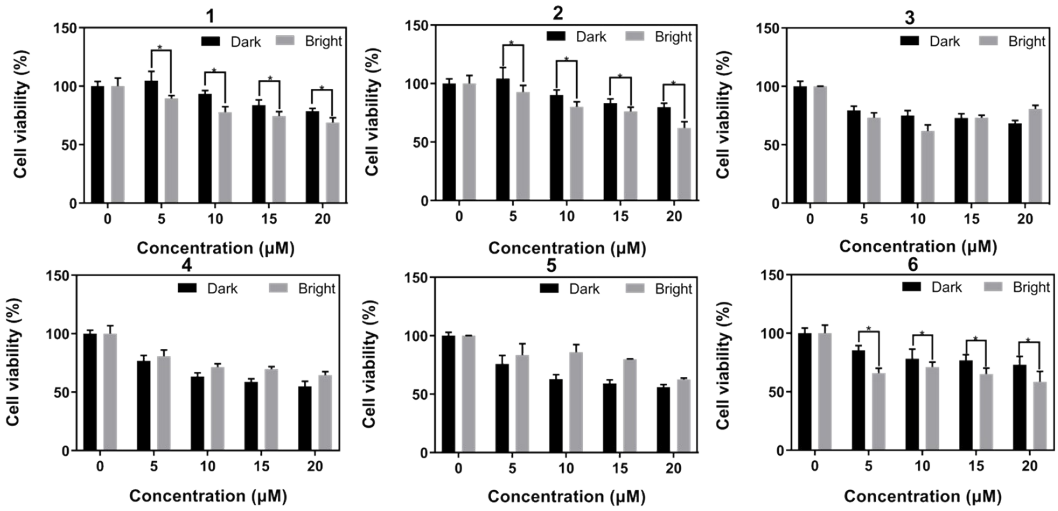

Fig. S22 Cell viability of HeLa cells incubated with complex **1** to **6**.

References:

1. W. J. Welch, *Physiol. Rev.*, 1992, **72**, 1063-1081.
2. D. Kültz, *Annu. Rev. Physiol.*, 2005, **67**, 225-257.